



## Optimizing hole-injection in organic electroluminescent devices by modifying CuPc/NPB interface

Meng-Dan Jiang<sup>a</sup>, Pei-Yu Lee<sup>b</sup>, Tien-Lung Chiu<sup>b,\*</sup>, Hong-Cheu Lin<sup>a,\*</sup>, Jiun-Haw Lee<sup>c</sup>

<sup>a</sup> Department of Materials Science and Engineering, National Chiao Tung University, Hsinchu, Taiwan, ROC

<sup>b</sup> Department of Photonics Engineering, Yuan Ze University, Taoyuan, Taiwan, ROC

<sup>c</sup> Graduate Institute of Photonics and Optoelectronics and Department of Electrical, Engineering, National Taiwan University, Taipei, Taiwan, ROC

### ARTICLE INFO

#### Article history:

Received 19 February 2011

Received in revised form 28 May 2011

Accepted 6 June 2011

Available online 23 July 2011

#### Keywords:

Organic light-emitting device

Remote pulsed Ar plasma

Hole-blocking

Layer

### ABSTRACT

This investigation discusses the performance of an organic light-emitting device (OLED) with ultraviolet (UV) illuminated and remote pulsed Ar plasma (RPAP), treated copper phthalocyanine (CuPc) thin film on an indium tin oxide anode as the hole-blocking layer. UV treatment increased the driving voltage, the current efficiency decreased at the same time due to the poor sticking probability of NPB on the CuPc surface. By contrast, the driving voltage reduction and current efficiency enhancement were achieved at the same time for the OLED with the RPAP treated CuPc. Besides this, in such device, the thickness of CuPc affects seldom the current density–voltage–luminance characteristics. The surface characteristics of these processed CuPc thin films were investigated by using atomic force microscope, contact angle and X-ray photoelectron spectroscopy measurements, which showed the CuPc/ N,N'-bis-(1-naphthyl)-N,N'-diphenyl-1,1'-biphenyl-4,4'-diamine (NPB) interface was crucial to not only the interface energy barrier, but also the following NPB growth, mode.

© 2011 Elsevier B.V. All rights reserved.

### 1. Introduction

Organic light emitting diodes (OLED) has attracted much attention for the applications as flat panel displays and lighting technology [1,2]. In such a device due to the heterojunction structure, the energy barriers at the interfaces determine the carrier injection performance of the OLED. Generally, several inorganic buffer layers are employed to eliminate this barrier by the chemical interaction of buffer layer and organic layer [3–6]. For organic buffer layer, copper phthalocyanine (CuPc) is a commonly used organic semiconductor with the favorable hole-transport property, high thermal stability, excellent adhesion and film-forming capacity which is used for the applications of OLEDs and organic solar cells [7,8]. As reported by Van Slyke et al. [9], with the inserting a CuPc to stabilize hole-injection contact for the hole-transporting layer (HTL) material, N,N'-diphenyl-N,N'-bis(1-naphthyl)-1,1'-biphenyl-4,4'-diamine (NPB), the driving voltage of OLED is reduced and the operation lifetime is elongated.

CuPc between ITO and HTL in OLED devices has been improved in several ways, such as by exploiting a graded interface [10,11], midgap states [12,13], sputter growth [14] and metal-free phthalocyanine (H<sub>2</sub>Pc)-doping [15]. However, Lee et al. and Hill and Kahn

verified the existence of a hole-transporting barrier from CuPc to NPB, which is around 0.4–0.5 eV [16,17]. Beierlein et al. used a thin red emitter as sensing layers to demonstrate that the CuPc/NPB interface limited the current flow at low voltage [18]. Therefore, a simple and reliable process must be developed to lower the energy barrier at the CuPc/NPB interface [11]. Hence, the pristine CuPc possessed hole-blocking characteristics [19], it is not the case that the hole-current overwhelms electron-one at the NPB/Alq<sub>3</sub> interface of device. Applying this hole-blocking layer were reported to prevent cationic Alq<sub>3</sub> formation and improve the device stability and lifetime [20,21]. On the other hand, with suitable device design, charge balance condition may be nearly satisfied [22].

The surface of organic materials is often modified by the plasma and ultraviolet (UV) radiation, which is absorbed via ionization, phonon excitation and atomic displacements [23,24]. Tong et al. demonstrated that the UV treatment of fluorocarbon (CF<sub>x</sub>), a buffer layer on anode improved the performance of OLED devices, whereas treatment with Ar ions caused atomic deterioration of CF<sub>x</sub> [24]. Atreya et al. found that electroluminescence (EL) would be substantially quenched in the plasma-treated samples [25]. Electrons, ions and UV in discharge plasma region typically directly attack the surfaces of organic materials, easily generating degradation products with low molecular weight and spikes on the harsh surfaces with high roughness. Such heavy etching and serious degradation, which damage the optical and electrical properties are also extremely undesirable [26].

\* Corresponding author. Tel.: +886 3 463 8800; fax: +886 3 451 4281.

E-mail addresses: [tchiu@saturn.yzu.edu.tw](mailto:tchiu@saturn.yzu.edu.tw) (T.-L. Chiu), [linhc@cc.nctu.edu.tw](mailto:linhc@cc.nctu.edu.tw) (H.-C. Lin).

**Table 1**

Contact angle and root-mean-square-roughness of CuPc films before and after RPAP- or UV-treatment.

Sample	Contact angle (°)	$R_{\text{rms}}$ (nm)
CuPc	60.18	2.27
UV-CuPc	67.16	1.72
RPAP-CuPc	32.05	2.16

In this work, an attempt is made to modify CuPc films using the moderate UV illumination and mild remote pulsed Ar plasma (RPAP) treatment. It showed surface roughness was nearly the same after the UV- and RPAP-treatments, which meant there was no obvious mechanical damage to the CuPc film. On the other hand, in contact angle measurement, it suggested that CuPc surface after UV and RPAP treatments became more hydrophobic and hydrophilic, respectively, which affected the sticking probability of NPB a lot. In device performances, it showed that RPAP-CuPc-OLED exhibited not only the lower driving voltage but also the higher current efficiency. Besides, device characteristics were nearly identical for various CuPc thicknesses, which increased the flexibility in device design and broadened the process window.

## 2. Experimental

In our OLED, CuPc, NPB, tris-(8-hydroxyquinoline) aluminum ( $\text{Alq}_3$ ), LiF, and Al are used as the hole-blocking layer (HBL), HTL, emitting layer, electron-injection layer, and cathode, respectively. The configuration of device structure was ITO substrate/CuPc (0–20 nm)/NPB (50 nm)/ $\text{Alq}_3$  (70 nm)/LiF (0.5 nm)/Al (200 nm). The active area of the EL device was typically  $0.04 \text{ cm}^2$ . The ITO substrate with a sheet resistance of  $13 \Omega/\square$  was used to fabricate the OLED, which was cleaned in acetone and isopropanol by ultrasonication, and dried in flowing nitrogen before being treated with the plasma generator (40 W, 10 min.). The ITO-coated substrates were deposited on a CuPc and then treated with UV and RPAP. The UV illumination (270–350 nm) was performed using a mercury lamp in a glovebox that was filled with 5 N pure nitrogen gas. The RPAP were conducted by using very mild Ar plasma with a low mean power input of 9 W in a vacuum chamber (300 mTorr). The samples were placed around 40 cm away from the active area to reduce the UV irradiation, ionic bombardment and etching. For OLED measurements, the current density–voltage–luminance (J–V–L) characteristics were obtained using a programmable Keithley model 237 power source and a Minolta spectrometer. An X-ray photoelectron spectroscopy (XPS), an atomic force microscope (AFM) and a contact angle meter were used to study the chemical modification, surface morphology and hydrophilic characteristics of the CuPc films, respectively.

## 3. Results and discussions

Table 1 presents the variations of contact angles and root-mean square roughness ( $R_{\text{rms}}$ ) for the CuPc layers treated with RPAP and UV irradiation. The RPAP-CuPc film was more hydrophilic than the pristine CuPc, as the contact angle was drastically reduced from  $60.18^\circ$  (wetting tension  $27 \text{ mN/m}$ ) to  $32.05^\circ$  (wetting tension  $62 \text{ mN/m}$ ) after a plasma-treatment period of 60 s; by contrast, the UV-CuPc film became hydrophobic, with a contact angle of  $67.16^\circ$  after a UV-illumination period of 60 s. Hill and Kahn observed by making UPS measurements that the NPB has a low probability of sticking on the CuPc surface [17]. Modification of the surface of the RPAP-CuPc layer to a hydrophilic surface (with a higher wetting tension) is expected to improve the NPB sticking probability on the CuPc surface, preventing island growth and promoting the adhesion of CuPc/NPB interface.

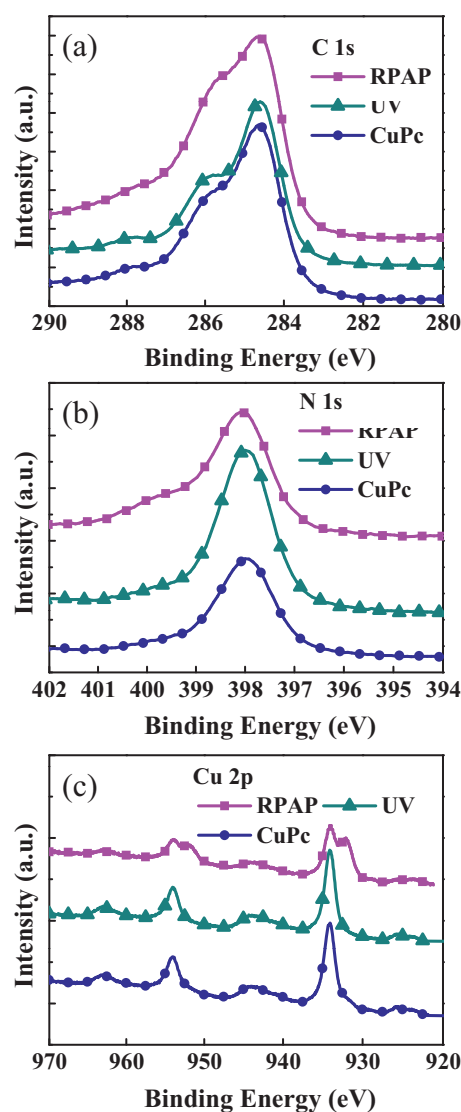


**Fig. 1.** XPS spectra of the CuPc, RPAP-CuPc and UV-CuPc films for (a) C(1S), (b) N(1S), and (c) Cu( $2P_{1/2}, 2P_{3/2}$ ), respectively.

In addition, the surface quality and morphology of these treated CuPc layers could be evaluated by  $R_{\text{rms}}$  from AFM images. In Table 1, the  $R_{\text{rms}}$  of CuPc, RPAP-CuPc and UV-CuPc were 2.27, 2.16, and 1.72 nm, respectively. The morphology of the RPAP-CuPc films was almost as rough as that of pristine CuPc. In contrast, the morphology of CuPc film gradually changed to a more homogenous and smoother film after a UV-illumination time of 60 s due to the rearrangement of surface CuPc molecular [27]. Hence, the roughnesses of these three films are approximate and can be served as good even quality. This means less probability of the defects or spikes generation at the organic interfaces, leading to short circuits and damages of their EL devices.

Fig. 1(a) shows the spectrum of the CuPc films for C 1s, which is similar to that obtained by Kim et al. and revealed two forms of carbon: 24 carbon atoms with aromatic hydrocarbons and eight carbon atoms bonded to two nitrogen atoms [14]. The aromatic carbons binding energy of CuPc was at 284.6 eV and C–N was at 285.5 eV. The corresponding peaks of the two forms of carbon for the CuPc, RPAP-CuPc, and UV-CuPc had relative intensity area ratios of about 2.03:1, 3.02:1, and 2.29:1, respectively. Since oxygen in the oxygen-plasma-treated ITO electrode may have diffused into the 10 nm CuPc film and the interaction between oxygen and copper, carbon

and nitrogen would have then resulted in getting non-consistent with the atomic ratio of the aromatic carbons and carbons with C–N. Interestingly, we observed that the UV-CuPc layer shows exact atomic ratio of all about 3:1, that means UV light illumination induced the desorption of O<sub>2</sub> from the CuPc surface. The oxidation peak at 286.3 eV (C–O) and 288 eV (C=O) was thought to be associated with the exposure of activated RPAP-CuPc sample to the atmosphere when they are transferred from the vacuum plasma chamber into the XPS analyzer, and the consequent diffusion of some of the O<sub>2</sub> and H<sub>2</sub>O that had been adsorbed by the sample into the CuPc, broadening the O 1s spectrum peak toward higher binding energy, since the oxygen of O<sub>2</sub> and H<sub>2</sub>O have higher binding energy.

Fig. 1(b) is the XPS spectrum of the CuPc films for N 1s, which shows that Cu–N bond was loosened in the RPAP-CuPc and UV-CuPc. The corresponding peaks of the two forms of N 1s, i.e. C–N=C bond at 398.3 eV and Cu–N bond at 397.7 eV, for the pristine CuPc, RPAP-CuPc, and UV-CuPc had relative intensity area ratios of about 1:1.26, 1:0.64, and 1:0.67, respectively. The O–C–N peak at 399.53 eV was thought to be associated with the exposure of activated RPAP-CuPc sample to the atmosphere when they were transferred from the vacuum plasma chamber into the XPS analyzer, and the consequent diffusion of some of the O<sub>2</sub> and H<sub>2</sub>O that had been adsorbed by the sample into the CuPc. Interestingly, the Cu–N bond of the UV-CuPc films appeared to be loosened, but had no activated UV-CuPc films to form an O–C–N bond.

Fig. 1(c) is the XPS spectrum of the CuPc films for Cu 2p, which shows the RPAP-CuPc film is clear different from the CuPc and UV-CuPc films. For all samples, the Cu(II) species with multiplet splitting satellite peaks were observed, which reflect the 3d<sub>x<sup>2</sup>-y<sup>2</sup></sub> orbital comprises in the molecular plane [28]. The corresponding peaks of the Cu 2p<sub>1/2</sub> at 954 eV and Cu 2p<sub>3/2</sub> at 934.1 eV for the CuPc, RPAP-CuPc, and UV-CuPc had relative intensity area ratios of about 1:2.28, 1:2.04, and 1:2.28, respectively. For the RPAP-CuPc film, the species of Cu(I) and Cu with multiplet splitting peaks were observed, which the corresponding peaks of the Cu 2p<sub>1/2</sub> at 952 eV and Cu 2p<sub>3/2</sub> at 932.2 eV had relative intensity area ratios of about 0.98:2.17.

Modifying a CuPc film using RPAP treatment can mildly activate its surface. Tong et al. demonstrated that bombarding argon ions penetrate the 2 nm-thick Cfx layer and modify the ITO as well [24]. Remote pulsed Ar plasma treatment can be used to modify the CuPc surface without damaging the bulk structure, as would occur by using UV, ion bombardment or etching. These findings may explain the favorable performance of a device with RPAP-CuPc.

The near-UV energy of 270–350 nm (3.6–4.6 eV) does not suffice to break the C=C bond (bond energy 6.35 eV) or the C=N bond (bond energy 9.26 eV) but only some of this energy is required to break  $\pi$  bonds (bond energy 2.74 eV), C–N bonds (bond energy 3.17 eV), C–O bonds (bond energy 3.74 eV) or C–C bonds (bond energy 3.61 eV). UV emission at 126 nm (9.84 eV) from Ar excimer in the direct Ar plasma zone is sufficient to break up CuPc molecules, markedly damaging the phosphine ring and the aromatic character. Accordingly, RPAP treatment was employed herein.

Fig. 2 shows the current density versus voltage and luminescence for devices fabricated with CuPc, RPAP-CuPc and UV-CuPc with thickness of 2 nm, namely device A, B and C. At 50 mA/cm<sup>2</sup>, their driving voltage were 9.23, 8.69, and 11.48 V, as well as luminescence were 2438, 2157 and 1514 nits for the device A, B and C as shown in Fig. 2, respectively. Evidently, the additional RPAP treatment effectively reduces the driving voltage due to the lowering of the energy barrier at CuPc/NPB interface induced the less return current and favored the injection of holes [19]. This return current did not contribute to light emission. For CuPc with RPAP case, the interface between CuPc/NPB was modified, there is less return current, which means the optimal number of hole can trans-

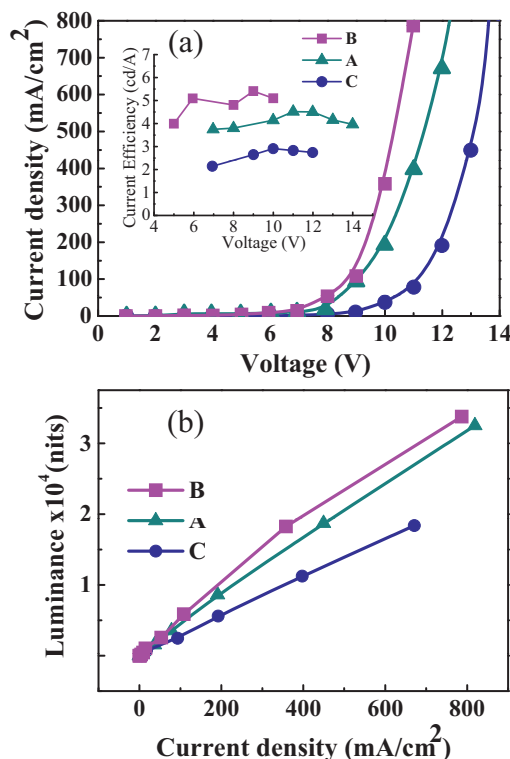
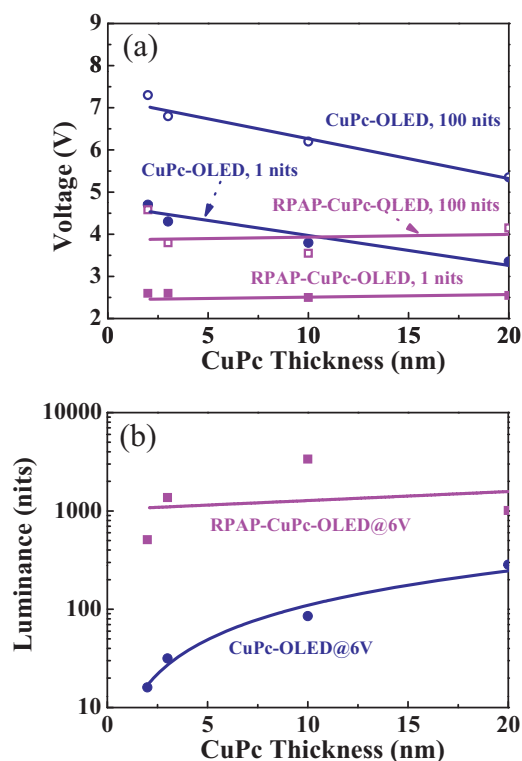


Fig. 2. (a) current density versus voltage, and (b) luminescence versus current density characteristics of the device A, B and C. The inset presents their current efficiency.

port through NPB layer and efficiently recombine with electron at NPB/Alq<sub>3</sub> interface to achieve the condition of charge balance. It resulted in a lower driving voltage and higher luminescence, compared with the CuPc without RPAP treatment. Corresponding to Fig. 2(b), RPAP treatment also benefits charge balance by electron and hole to emit a higher luminescence of 2438 nits at 50 mA/cm<sup>2</sup>.

The inset of Fig. 2(a) shows the current efficiency (in terms of cd/A) versus voltages for these three devices. Compared with device A, device B can note that RPAP treatment increases the efficiency obviously and its maximum efficiency is 5.41 cd/A@9V. On the other hand, OLED with CuPc HBL treated by UV illumination results in a lower efficiency, like device C. In our measurement, we also observed the luminescence nonuniformity in the pixel of the device C, which may cause from the hydrophobic effects on the surface of CuPc. Although the uniformity of CuPc was quite good (i.e.  $R_{\text{rms}} = 1.72$  nm, as shown in Table 1), the sticking probability of NPB on the CuPc surface was reduced due to the high contact angle (i.e. 67.16°, as shown in Table 1), which resulted in a low current efficiency.

Fig. 3(a) shows the driving voltages at 1 and 100 nits, respectively, for the OLEDs with various thicknesses of CuPc and RPAP-CuPc HBLs. One can clearly see the driving voltages of RPAP-CuPc-OLEDs are lower than that of CuPc-OLEDs. Besides, for the CuPc-OLEDs, driving voltage reduces with increasing CuPc thickness due to the reduction of the return current at the CuPc/NPB interface [19]. The thick CuPc thickness prevents the oxygen diffusion from ITO to CuPc/NPB interface. Oxygen results in the increase barrier at the CuPc/NPB interface and larger return current. Hence, the thicker CuPc thickness causes to less return current, benefitting the hole-injection at this interface. By contrast, for RPAP-CuPc-OLEDs, the driving voltage is insensitive to the CuPc thicknesses, because RPAP-treatment only modified CuPc surface and in turns facilitates the hole-injection capability. Hence, CuPc/NPB interface barriers, rather than charge-carrier transport, limit the current at low voltage in our case. Fig. 3(b) shows the luminescence at 6 V for



**Fig. 3.** (a) Driving voltage at 1 and 100 cd/m<sup>2</sup>, and (b) luminescence at 6V for the cases of CuPc-OLED and RPAP-CuPc-OLED with different CuPc thicknesses.

the cases of CuPc- and RPAP-CuPc-OLEDs. The luminance of CuPc-OLEDs increases with thicker CuPc thickness. RPAP-CuPc-OLED always exhibits high luminance than CuPc-OLED under constant voltage driving and its luminance is insensitive to CuPc thickness. In addition, CuPc cannot only act as the HBL, but also impedes oxygen diffusion into organic layers for elongating operation lifetime [9]. Consequentially, the RPAP-CuPc-OLED is expected to perform the more reliable and provide more flexibility in device design.

#### 4. Conclusions

In summary, the RPAP-CuPc layer significantly improved device performance such as voltage reduction and efficiency enhancement, which was achieved by modifying the CuPc film surface to make it hydrophilic without heavy etching or serious degradation, thereby strengthening CuPc/NPB interface adhesion, reducing the return hole-current, optimizing hole-injection, reducing the operating voltage, and retaining the ITO/CuPc ohmic contact. Surface

modification of the UV-CuPc layer to make its surface hydrophobic (with a low wetting tension) was thought to reduce the probability of NPB sticking to the CuPc surface, weakening CuPc/NPB interface adhesion.

#### Acknowledgments

The authors would like to thank National Science Council (NSC) and Chung-Shan Institute of Science and Technology (CSIST) of Taiwan for financial support under grant nos., NSC 98-2221-E-002-038-MY3, 99-2622-E-155-010-CC3, 99-2221-E-155-092, and 99-2218-E-155-003 as well as using the facilities in CSIST.

#### References

- [1] C.W. Tang, S.A. Vanslyke, *Appl. Phys. Lett.* 51 (1987) 913–915.
- [2] T.L. Chiu, P.Y. Lee, C.H. Hsiao, M.K. Leung, C.Y. Chen, C.C. Yang, J.H. Lee, *J. Appl. Phys.* 109 (2011) 084520.
- [3] C.I. Wu, C.T. Lin, G.R. Lee, T.Y. Cho, C.C. Wu, T.W. Pi, *J. Appl. Phys.* 105 (2009) 033717.
- [4] M.Y. Chan, S.L. Lai, M.K. Fung, C.S. Lee, S.T. Lee, *J. Appl. Phys.* 95 (2004) 5397–5402.
- [5] L. Niu, Y. Guan, *Phys. Status Solidi A* 207 (2010) 993–997.
- [6] T.L. Chiu, W.F. Xu, C.F. Lin, J.H. Lee, C.C. Chao, M.K. Leung, *Appl. Phys. Lett.* 94 (2009) 13307.
- [7] S. Rajaputra, G. Sagi, V.P. Singh, *Sol. Energy Mater. Sol. Cells* 93 (2009) 60–64.
- [8] C.F. Lin, M. Zhang, S.W. Liu, T.L. Chiu, J.H. Lee, *Int. J. Mol. Sci.* 12 (2011) 476–505.
- [9] S.A. Van Slyke, C.H. Chen, C.W. Tang, *Appl. Phys. Lett.* 69 (1996) 2160–2162.
- [10] H. Riel, S. Barth, T. Beierlein, W. Brütting, S. Karg, P. Müller, W. Riefl, *SPIE* 4105 (2001) 167–174.
- [11] S.M. Tadayyon, H.M. Grandin, K. Griffiths, P.R. Norton, H. Aziz, Z.D. Popovic, *Org. Electron.* 5 (2004) 157–166.
- [12] G. Parthasarathy, P.E. Burrows, V. Khalfin, V.G. Kozlov, S.R. Forrest, *Appl. Phys. Lett.* 72 (1998) 2138–2140.
- [13] S. Steil, K. Goedel, A. Ruffing, I. Sarkar, M. Cinchettia, M. Aeschlimanna, *Synth. Met.* (2011), doi:10.1016/j.synthmet.2010.11.031.
- [14] S.C. Kim, G.B. Lee, M.W. Choi, Y. Roh, C.N. Whang, K. Jeong, J.G. Lee, S. Kim, *Appl. Phys. Lett.* 78 (2001) 1445–1447.
- [15] T. Mori, T. Mitsuoka, M. Ishii, H. Fujikawa, Y. Taga, *Appl. Phys. Lett.* 80 (2002) 3895–3897.
- [16] S.T. Lee, Y.M. Wang, X.Y. Hou, C.W. Tang, *Appl. Phys. Lett.* 74 (1999) 670–672.
- [17] I.G. Hill, A. Kahn, *J. Appl. Phys.* 86 (1999) 2116–2122.
- [18] T.A. Beierlein, B. Ruhstaller, D.J. Gundlach, H. Riel, S. Karg, C. Rost, W. Riefl, *Synth. Met.* 138 (2003) 213–221.
- [19] Y. Divayana, B.J. Chen, X.W. Sun, T.K.S. Wong, K.R. Sarma, X. Hu, *J. Cryst. Growth* 288 (2006) 105–109.
- [20] H. Aziz, Z.D. Popovic, N.X. Hu, A.M. Hor, G. Xu, *Science* 283 (1999) 1900–1902.
- [21] Z.D. Popovic, H. Aziz, N.X. Hu, A.M. Hor, G. Xu, *Synth. Met.* 111 (2000) 229–232.
- [22] Z.D. Popovic, H. Aziz, *IEEE J. Quant. Electron.* 8 (2002) 362–371.
- [23] S. Miyata, Y.H. Park, Y. Soeda, R. Itoh, S. Tasaka, *Jpn. J. Appl. Phys.* 26 (1987) L11632.
- [24] S.W. Tong, C.S. Lee, Y. Lifshitz, D.Q. Gao, S.T. Lee, *Appl. Phys. Lett.* 84 (2004) 4032–4034.
- [25] A. Atreya, S. Li, E.T. Kang, K.G. Neoh, K.L. Tan, *Polym. Degrad. Stab.* 63 (1999) 53–59.
- [26] C.F. Lin, S.W. Liu, W.F. Hsu, M. Zhang, T.L. Chiu, Y. Wu, J.H. Lee, *J. Phys. D: Appl. Phys.* 43 (2010) 395101.
- [27] L.A. Peyser, T.H. Lee, R.M. Dickson, *J. Phys. Chem. B* 106 (2002) 7725–7730.
- [28] F. Rochet, G. Dufour, H. Roulet, N. Motta, A. Sgarlata, M.N. Prancastelli, M. DeCrescenzi, *Surf. Sci.* 319 (1994) 10–20.